

J. Synchrotron Rad. (1999). **6**, 537–539

XMCD and magnetism of the ferrimagnetic system $\text{NaV}_6\text{O}_{11}$

^(a)E. Goering, ^(a)D. Ahlers, ^(a)K. Attenkofer, ^(b)G. Obermeier, ^(b)S. Horn und ^(a)G. Schütz

^(a)*Lehrstuhl für Experimentalphysik IV, Universität Würzburg: goering@physik.uni-wuerzburg.de*

^(b)*Lehrstuhl für Experimentalphysik 2, Universität Augsburg*

We investigated the XMCD signal at the $V L_{2,3}$ - and the O K- edges. Sum rules exhibit that $\text{NaV}_6\text{O}_{11}$ is mainly a spin magnet with a small contribution of an orbital moment, but due to the small spin-orbit splitting of the $V L_{2,3}$ -edges a direct extraction of the magnetic moment is problematic. We can identify two antiferromagnetically coupled sub bands. Ferromagnetic correlations were observed along one direction. The electronic transport properties are dominated along the easy axis in the canted ferrimagnetic low temperature structure

Keywords: transition metal oxides; x-ray magnetic circular dichroism; ferrimagnetism

1. Introduction

In oxides antiferromagnetism is much more common than ferromagnetism. Most transition metal oxides show semiconducting or insulating behavior in correlation with antiferromagnetism. This behavior has been described by a Mott-Hubbard type insulator in the limit of $U/W \approx \infty$ which results in an antiferromagnetic superexchange (Mott 1990). Ferromagnetism was found in very few systems. Most of the known ferromagnetic systems show metallic behavior, such as CrO_2 , SrCoO_3 or SrRuO_3 . However ferromagnetic semiconductors like EuO and EuS were also found. The discovery of the 'colossal magneto resistance' in the $\text{La}_{1-x}\text{M}_x\text{MnO}_3$ ($M=\text{Sr},\text{Ca}$) system gained growing interest in magnetism and electronics. CMR has an extremely high potential for technical applications such as data storage devices, spin-transistors, etc. Nevertheless correlations of magnetic and electronic transport properties in oxides are also very important in theoretical physics (Khomskii 1997). For a quantitative description of these systems it is necessary to separate the influence of lattice distortions (Jahn-Teller), correlation effects and magnetism. XAFS spectroscopy provides a unique technique to separate these effects in an element specific way. The unoccupied band structure could be separated by means of energy, symmetry, spin- and orbital moments.

The highly distorted system $\text{NaV}_6\text{O}_{11}$ shows ferromagnetic behavior which is strongly correlated with electronic transport properties. In the high temperature phase above 245K three different V-sites are present. Two sites are octahedrally surrounded by oxygen with a nominal valence of $V(1)^{3+}$ and $V(2)^{4+}$, respectively. The third V-site $V(3)^{3+}$ is situated inside a trigonal bipyramid. The relative ratio is found to be $V(1):V(2):V(3) = 3:2:1$ (Kanke 1992). At temperatures above 245K $\text{NaV}_6\text{O}_{11}$ is paramagnetic, belongs to the hexagonal spacegroup $P6_3/mmc$, shows a linear χ^1 behavior and has an

effective magnetic moment of $2.0\mu_B$ (Uchida 1991). Below 245K the symmetry is reduced to the hexagonal spacegroup $P6_3mc$. A second structural phase transition occurs at 35K. Below 35K the symmetry reduces to the orthorhombic spacegroup $\text{Cmc}2_1$. The Curie temperature is $T_c=64$ K. Below 120K the magnetic susceptibility is anisotropic. χ^1 along [001] shows an effective magnetic moment of $1.1\mu_B/\text{V-ion}$ between 75K and 110K. In the ferromagnetic region below 64K the system has a uniaxial ferromagnetic anisotropy along the [001] direction. At 5K the saturation magnetization results in a magnetic moment per formula unit of $1.7\mu_B$ which corresponds to a small magnetic moment of $0.28\mu_B/\text{V-ion}$.

The electrical resistivity is strongly anisotropic. Along the [001] direction the system exhibits metallic behavior in the whole temperature region. Perpendicular to the [001] direction the temperature dependence is more complicated. Below T_c and above 245K the behavior is metallic whereas it is semiconducting in between (Uchida 1991).

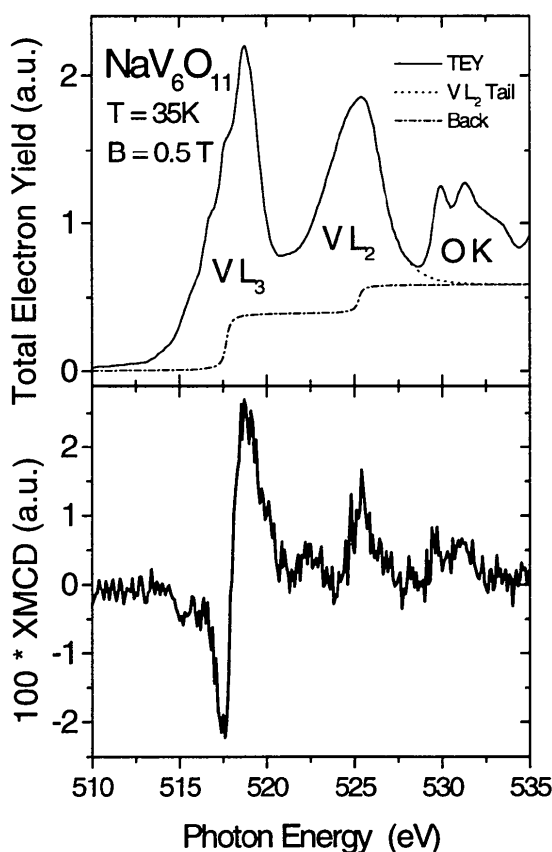


Figure 1
XAS (above) and XMCD of $\text{NaV}_6\text{O}_{11}$ at the $V L_{2,3}$ - and O K-edges

2. Experimental Procedures

Polycrystalline samples were prepared by solid state reaction. High purity powders of NaVO_3 , V_2O_3 and V_2O_5 were used. The procedure is very similar to that described by (Kanke 1990). Samples were characterized by x-ray diffraction and magnetic

susceptibility measurements. No spurious phases were detected. Details of sample preparation and characterization are described elsewhere (Obermeier 1996).

XMCD spectra were recorded at the PM3 (SX-700 III) monochromator at BESSY I. The energy width of the monochromatic synchrotron beam was about 0.7 eV at the V $L_{2,3}$ - and O K-edges. A superconducting UHV magnet system was used and the applied magnetic field was 0.5T. For each energy point the magnetic field was flipped in a [+ -] and [- +] sequence to minimize systematic errors. Spectra were taken in the Total-Electron-Yield mode (TEY) measuring the total drain current. The measured photocurrent lies between 1-10pA. The noise level of the system was reduced to 5fA by using dedicated Keithley triaxial low noise cables and Keithley 617 electrometers. To minimize additional noise no voltages were applied to increase the total drain current at an applied magnetic field.

Throughout the measurement the sample temperature was kept at 35K.

In Fig. 1 the total electron yield spectra for two different magnetic

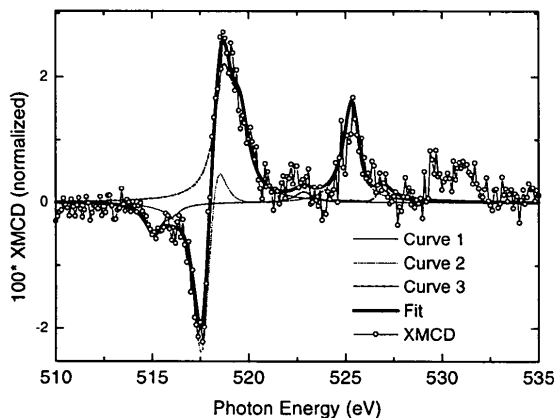


Figure 2
XMCD Spectra and fit of $\text{NaV}_6\text{O}_{11}$; Three sub-spectra curve 1-3

field directions and their difference are shown. The spectra were normalized to the total edge jump of all three edges. The energy was calibrated, so that the first peak at the O K-edge is positioned at 530eV (Goering 1994). To separate the V- and the O- contributions to the XAS spectra the high energy tail of the V L_2 -edge was fitted with an exponential decay. This is indicated by the dotted curve. For an estimation of the white line intensity a double arctan (517.7eV, 525.2eV; ratio 2:1) with a 10%-90% width of 1eV was used (Chen 1995). A very small XMCD effect is visible (about 1% compared to the white line intensity).

3. Discussion

A qualitative comparison exhibits similarities between the XMCD spectra and V/Fe-multilayer spectra (Harp 1995)(O'Brien 1994). Nevertheless the XMCD spectra show more details. Harp (Harp 1995), O'Brien (O'Brien 1994) and Wu (Wu 1993) pointed

out problems using sum rules in transition metal compounds with a small LS-coupling in the p core hole state. Additionally one expects more complicated spectra in $\text{NaV}_6\text{O}_{11}$, because two different nominal Vanadium valences (V^{3+} and V^{4+}) and five different V-sites are present in the low temperature phase. Antiferromagnetic coupling and energy splitting due to solid state effects should result in very complicated XMCD spectra. Gerrit Van der Laan (Laan 1997, 1997b) uses a sum of various ground state moments to obtain a qualitative agreement with the behavior of the XMCD TM series (O'Brien 1994).

To extract different contributions to the observed XMCD-spectrum of $\text{NaV}_6\text{O}_{11}$, the XMCD-spectrum is fitted with a sum over three different curves. Fitting the data with a small number of ground state moments we minimize the degrees of freedom. Only three different moments are used. The first one is the \underline{w}^{000} -moment, which is proportional to the number of holes n_h . The second one is the \underline{w}^{011} -moment, which is proportional to the spin magnetic moment S_z . The third one finally is the \underline{w}^{101} -moment, which is proportional to the orbital magnetic moment L_z . The result of this fit is shown in Fig. 2.

The XMCD spectrum is perfectly described by the fit. The LS-coupling of the core level was fixed to 7.56 eV (7.7 for V-metal (Fuggle 1980)), which is a mean value obtained previously by XPS-measurements (not shown) on various Vanadium oxides (Zimmer 1998). Three different energy levels were used. Every energy level corresponds to a single curve. The energy position of each curve is given in Table 1.

Table 1

| | Curve 1 | Curve 2 | Curve 3 |
|--------------------------|---------|---------|---------|
| Center of L3-Energy (eV) | 515.5 | 518 | 519.1 |

The effective exchange coupling energy of the 3d electrons and the core holes was estimated by $H_s=0.9\text{eV}$ (cf. (Laan 1997b)) and for best agreement with experimental XMCD data the width of the Lorentzians was set to 1.05eV to take band structure and lifetime broadening effects into account.

In Fig.3 all three curves and their corresponding ground state moment spectra are shown. The little pre-peak (515eV) and the peak in the middle region (522.5eV) originate from curve 1. Curve 2 dominates the spectrum at 517.5eV and 525.3eV. Curve 3 dominates the high energy shoulder of the L_3 - and the L_2 -edges and is dominated by the orbital momentum. It is clearly antiferromagnetically coupled to curve 2.

Sum rules have been applied to these spectra (Thole 1992)(Carra 1993). The procedure is nearly the same as was the one previously followed for Fe (Chen 1995). By means of the fitting, however, problems with overlapping $L_{2,3}$ -features could be avoided. To extract the white line intensity, the O K-edge contribution at the high energy tail of the L_2 -edge and the background were subtracted as shown in Fig. 1. The average number of core holes n_h was simply estimated to be 8.5, corresponding to an average valence of $\text{V}^{3.5+}$. Up to now no theoretical value for n_h is available. The difference in saturation magnetization at 35K and 5K was corrected for by a factor of $1.064=M(5K)/M(35K)$. The degree of circular polarization was 76%. No self absorption was corrected, which is problematic for powder samples. The total spin moment was $S_z = 0.043 \mu_B$ and the total orbital moment was $L_z = -0.030 \mu_B$. The observed magnetic anisotropy is a result of the large orbital moment. The L_z/S_z ratio is

quite enhanced. This may be explained in terms of reduced hybridization and bandwidth in oxides. Additional V-Ions 'feel' an orthorhombic crystal field and not a cubic one. Therefore some parts of the orbital momentum may be preserved from quenching.

The above values for S_z and L_z disagree with the corresponding measurements of the low temperature values of $0.28\mu_B$ (Uchida 1991). This discrepancy can be understood as follows. The white line intensity originates from both magnetic and nonmagnetic ions whereas the XMCD spectra are purely ferromagnetic. Application of sum rules implies the ratio of XMCD

(Uchida 1991). If the system is purely ferrimagnetic, the white line intensity has to be reduced by a factor of $2.0\mu_B / 0.28\mu_B = 7.14$. Taking this reduction into account we get a total spin-moment of $S_z = 0.303\mu_B$ and a total orbital moment of $L_z = -0.22\mu_B$. Further analysis of each curve and a detailed comparison with a standard ferrimagnet like $\text{Eu}_3\text{Fe}_5\text{O}_{12}$ will be presented elsewhere.

3. Conclusions

$\text{NaV}_6\text{O}_{11}$ could be clearly identified as a ferrimagnet. Two major spectral contributions could be identified (curve 2 and 3). A large orbital moment was observed which is the origin of the magnetocrystalline anisotropy. A new technique ('momentum analysis') was developed to analyze complicated XMCD spectra with a small LS-coupling separation of the $L_{2,3}$ -edges. Using 'momentum analysis', sum rules could be used for ferrimagnetic systems. The O K-edge XMCD could be unambiguously separated by means of the fitting procedure.

We would like to thank the BESSY beamline staff Heiko Gundlach for support and help. This project is funded by the BMBF and the DFG Forschergruppe TP2 Augsburg.

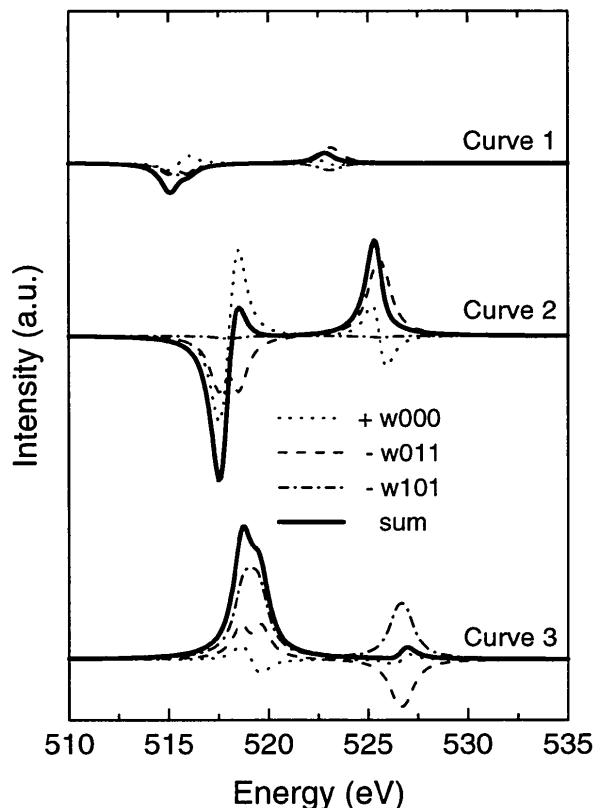


Figure 3
Three different curves and corresponding momentum distributions

spectra to their 'corresponding' white line intensity. A simple ferrimagnet consists of a sum of two sublattices. The ions of each sublattice are ferromagnetically coupled while the two sublattices are coupled antiferromagnetically to each other. If there is no spectral energy separation of the two sublattice contributions, only the difference of the two submagnetizations results in XMCD spectral weight whereas the white line has contributions of all ions. Therefore the derived momentum is much too small. The low temperature phase of $\text{NaV}_6\text{O}_{11}$ is not clearly identified as to be either a ferrimagnetic state with high magnetic moments at each V site or as a ferromagnet with only small moments. If the system is a ferromagnet, the full magnetic moments should be observed. If, on the other hand, the coupling is antiferromagnetic, the deduced moment should be strongly reduced. The room temperature moment of $\text{NaV}_6\text{O}_{11}$ is $2.00\mu_B$ and the low temperature moment is $0.28\mu_B$

References

- Carra, P.; B. T. Thole, M. Altarelli and X. Wang (1993). *Phys. Rev. Lett.* **70**, 694
- Chen, C.T., Y. U. Idzerda, H.-J. Lin, N.V. Smith, G. Meigs, E. Chaban, G. H. Ho, E. Pellegrin and F. Sette (1995). *Phys. Rev. Lett.* **75**, 152-155
- Fuggle, J. C. and N. Mårtensson (1980). *J. Electron Spectrosc. Relat. Phenom.* **21**, 275; or <http://xray.uu.se/hypertext/EBindEnergies.html>
- Goering, E.; Mueller, O.; denBoer, M. L.; Horn, S. (1994). *Physica B* **194-196**, 1217-1218
- Harp G. R., S. S. P. Parkin, W. L. O'Brien, B. P. Tonner (1995). *Phys. Rev. B* **51**, 3293-3296
- Kanke, Y.; Takayama-Muromachi, E.; Kato, K.; Matsui, Y. (1990). *Journal of Sol. State Chem.* **89**, 130-137
- Kanke, Y.; Kato, K.; Takayama-Muromachi, E.; Isobe, M. (1992). *Acta Cryst. Sect. C* **48** (8), 1376-1380
- Khomskii D. I. and G. A. Sawatzky (1997). *Sol. State Comm.* **102**, 87-99
- Mott, N. F. (1990). *Metal-Insulator-Transitions 2nd ed.*, Taylor & Francis
- Obermeier, G. (1996). *Diploma Thesis, Augsburg 1996*
- O'Brien, W. L.; B. P. Tonner, G. R. Harp, S. S. Parkin (1994). *J. Appl. Phys.* **76**, 6462-6464
- Thole, B. T., P. Carra, F. Sette, and G. van der Laan (1992). *Phys. Rev. Lett.* **68**, 1943
- Uchida, Y.; Kanke, Y.; Takayama-Muromachi, E.; Kato, K. (1991). *Journal of the Physical Society of Japan*, **60**, 2530-2533
- Laan, Gerit van der (1997). *J. Phys. Condens. Matter* **9**, L259-L256
- Laan, Gerit van der (1997). *Phys. Rev. B* **55**, 8086-8089
- Wu, R., D. Wang, and A. J. Freeman (1993). *Phys. Rev. Lett.* **71**, 3581
- Zimmermann, R., Claessen, R., Reinert, F., and Hüfner, S., *J. Phys.: Condens. Matter* **10** (1998) p. 5697-5716

(Received 10 August 1998; accepted 14 December 1998)